Formation Mechanism of CaS-Bearing Inclusions and the Rolling Deformation in Al-Killed, Low-Alloy Steel with Ca Treatment

GUANG XU, ZHOUHUA JIANG, and YANG LI

The existing form of CaS inclusion in Ca-treated, Al-killed steel during secondary refining process was investigated with scanning electron microscopy and an energy-dispersive spectrometer (EDS). The results of 12 heats industrial tests showed that CaS has two kinds of precipitation forms. One form takes place by the direct reaction of Ca and S, and the other takes place by the reaction of CaO in calcium aluminates with dissolved Al and S in liquid steel. Thermodynamic research for different precipitation modes of CaS under different temperature was carried out. In particular, $CaO-Al_2O_3-CaS$ isothermal section diagrams and component activities of calcium aluminates were calculated by the thermodynamic software FactSage. By thermodynamic calculation, a precipitation-area diagram of oxide-sulfide duplex inclusion was established by fixing the sulfur content. The quantity of CaS, which was precipitated in a reaction between [Al], [S] and (CaO), can be calculated and predicted based on the precipitation-area diagram of oxide-sulfide duplex inclusion. Electron probe microanalysis and EDS were used for observing rolling deformation of different types of CaS-bearing inclusions during the rolling process. Low modification of calcium aluminates wrapped by CaS has different degrees of harm to steel in the rolling process. A thick CaS layer can prevent some fragile calcium aluminates from being crushed during the rolling process. Some oxide-sulfide duplex inclusion contains little CaS performed better deformation during the rolling process, but when CaS in oxide-sulfide duplex inclusion becomes more, it will cause the whole inclusion to lose plastic yielding ability. The plastic deformation region of CaS-bearing inclusion in a $CaO-Al_2O_3-CaS$ isothermal section diagram is confirmed.

DOI: 10.1007/s11663-016-0695-9

I. INTRODUCTION

CALCIUM treatment is widely used for inclusion modification in Al-killed steel. It makes the inclusions modify liquid globular calcium aluminates, which are easier to float up and to be absorbed by top slag, thereby improving the cleanness of steel. Although calcium has good modification ability to the inclusion in Al-killed steel, improper calcium treatment will bring adverse effects. Insufficient calcium treatment promotes the inclusion into solid calcium aluminates, which are hard to be removed. For excessive calcium treatment, redundant calcium will react directly with sulfur to form CaS inclusion. At the same time, the dissolved aluminum and sulfur in molten steel will react with CaO in excessive modification of calcium aluminates to form oxide-sulfur duplex inclusion, so that a large number of CaS-bearing inclusions will form after excessive calcium treatment. CaS-bearing inclusions can degrade the castability of steel on account of its high melting point and lead to erosion of the ladle slide gate as well as refractory nozzles during casting.[1] Several researchers have examined the formation mechanism of oxide-sulfide duplex inclusion and its rolling performance. Ye *et al.*[2] considered that dissolved aluminum and sulfur can react with CaO in complete or overmodified aluminum inclusion due to its high activity of CaO. Holappa *et al.*[3] pointed out that CaS and oxide-sulfide duplex inclusion is promoted by enrichment of sulfur in the liquid residual as well as by the decreasing of temperature. Choudary and Ghosh[4] established a thermodynamic model to forecast the formation of oxide-sulfide duplex inclusion generated from the reaction between [Al], [S] and liquid calcium aluminates in Al-killed steel. However, thermodynamic investigations of them only aimed at the Al-S equilibriums of CA, $C_{12}A_7$, and C_3A (where A means Al_2O_3 and C means CaO) for the precipitation of CaS in oxide-sulfide duplex inclusion. The authors of this article thinks that Al-S equilibriums of CA, $C_{12}A_7$, and C_3A alone cannot forecast the precipitation of CaS accurately because the a_{CaO} of each calcium aluminate is different and they should not be replaced by the a_{CaO} of CA, $C_{12}A_7$, or C_3A. It is worth mentioning that the research about how much CaS can be produced by the reaction between [Al], [S] and (CaO) is scarcely reported in the published literature. Jing Guo *et al.*[5] found that oxide-sulfide duplex inclusion has good rolling

GUANG XU, Doctoral Candidate, and ZHOUHUA JIANG and YANG LI, Professors, are with the School of Materials and Metallurgy, Northeastern University, 241 Mailbox, No. 3-11, Wenhua Road, Heping District, Shenyang, 110819, P.R. China. Contact e-mail: jiangzh263@163.com
Manuscript submitted March 10, 2016.
Article published online May 26, 2016.

performance. But when CaS in the oxide-sulfide inclusion increases, its rolling performance may become worse. Some CaS-bearing inclusions contain low modification of core that were not researched extensively in their study, so it is difficult to reveal the change law of the deformation of CaS-bearing inclusions during the rolling process.

In the present work, the thermodynamics for different precipitation methods of CaS under different temperatures and deformation behaviors of various types of CaS-bearing inclusions during the rolling process were studied. In particular, more calcium aluminates were considered in thermodynamic calculation of Al-S equilibrium and Ca-Al equilibrium. One kind of precipitation-area diagram for oxide–sulfur duplex inclusion was established by combining Al-S equilibrium with Ca-Al equilibrium under the condition of fixing sulfur content. For explaining the formation mechanism of oxide-sulfide duplex inclusion, an unreacted core model of evolution of the $CaO\text{-}Al_2O_3$ system into the $CaO\text{-}Al_2O_3\text{-}CaS$ system was established. Furthermore, the mass fraction of CaS precipitated in the reaction between [Al], [S] and (CaO) can be calculated based on the precipitation-area diagram and the model. Verification tests were carried out, and the results were in good agreement with the thermodynamic calculation. Change law of rolling performances for CaS-bearing inclusions during the rolling process were summarized by observing different CaS-bearing inclusions, and it was explained by thermodynamics with the help of the thermodynamic software FactSage. The plastic deformation region of oxide–sulfide duplex inclusion is roughly confirmed.

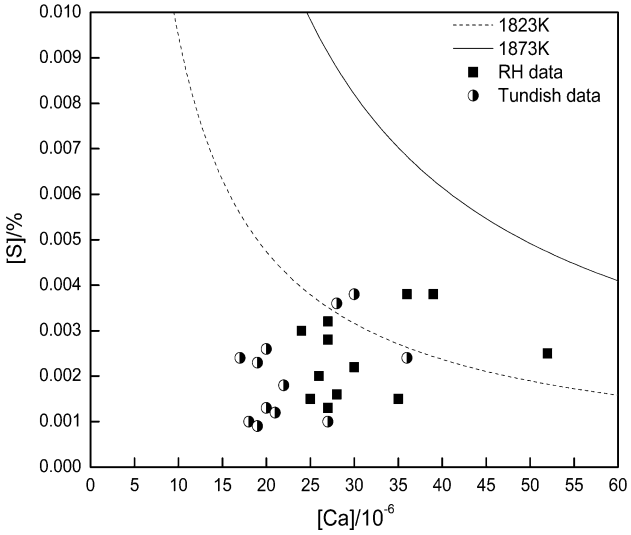

Fig. 1—Relationship between Ca and S for the precipitation of CaS.

Table I. Chemical Composition of Liquid Steel, Mass Percent

Station	C	Si	Mn	P	Ni
RH after calcium treatment	0.04 to 0.045	0.15 to 0.20	1.70 to 1.80	0.01 to 0.015	1.8 to 2.2
Tundish	0.04 to 0.045	0.15 to 0.20	1.70 to 1.80	0.01 to 0.015	1.8 to 2.2
Casting slab	0.04 to 0.045	0.15 to 0.20	1.70 to 1.80	0.01 to 0.015	1.8 to 2.2

Table II. Contents of S, Ca and Al_S in Liquid Steel, Mass Percent

Heats	1	2	3	4	5	6	7	8	9	10	11	12
S_{RH}	0.0020	0.0015	0.0025	0.0015	0.0032	0.0030	0.0028	0.0016	0.0038	0.0022	0.0013	0.0038
$S_{Tundish}$	0.0013	0.0010	0.0024	0.0010	0.0026	0.0024	0.0023	0.0012	0.0038	0.0018	0.0009	0.0036
S_{slab}	0.0013	0.0009	0.0016	0.0010	0.0020	0.0020	0.0019	0.0011	0.0027	0.0016	0.0008	0.0026
Ca_{RH}	0.0026	0.0035	0.0052	0.0025	0.0027	0.0024	0.0027	0.0028	0.0039	0.0030	0.0027	0.0036
$Ca_{Tundish}$	0.0020	0.0027	0.0036	0.0018	0.0020	0.0017	0.0019	0.0021	0.0030	0.0022	0.0019	0.0028
Ca_{slab}	0.0005	0.0008	0.0020	0.0004	0.0005	0.0006	0.0006	0.0006	0.0007	0.0006	0.0004	0.0011
Al_{sRH}	0.0450	0.0480	0.0450	0.0420	0.0390	0.0440	0.0410	0.0430	0.0440	0.0460	0.0420	0.0450
$Al_{sTundish}$	0.0440	0.0470	0.0460	0.0430	0.0400	0.0460	0.0400	0.0410	0.0450	0.0450	0.0440	0.0460
Al_{sslab}	0.0420	0.0450	0.0430	0.0410	0.0390	0.0440	0.0400	0.0400	0.0440	0.0430	0.0440	0.0450

Table III. First order Interaction Coefficients Used in Thermodynamic Calculation at 1823 K and 1873 K (1550 °C and 1600 °C)[6,8]

	j							
i	C	Si	Mn	Ni	P	S	Al	O
$S_{1873K(1600°C)}$	0.11	0.063	−0.026	0	0.29	−0.029	0.035	−0.27
$Al_{1873K(1600°C)}$	0.091	0.0056	0.0065	—	0.033	0.03	0.045	−6.6
$Ca_{1873K(1600°C)}$	−0.34[9]	−0.097	−0.0156[10]	−0.044	−0.097	−336[11]	−0.072[9]	−9000[12]
$S_{1823K(1550°C)}$	0.11*	0.063*	−0.026*	0*	0.29*	−0.031[13]	0.035*	−0.27*
$Al_{1823K(1550°C)}$	0.091*	0.0056*	0.0065*	—	0.033*	0.03*	0.046[13]	−7.11[13]
$Ca_{1823K(1550°C)}$	−0.34*	−0.097*	−0.0156*	−0.044*	−0.097*	−336*	−0.072*	−9000*

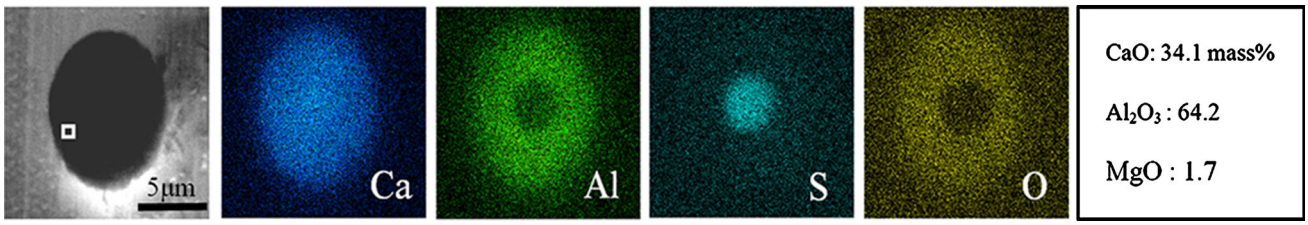

Fig. 2—SEM mapping of CaS wrapped by calcium aluminates after calcium treatment.

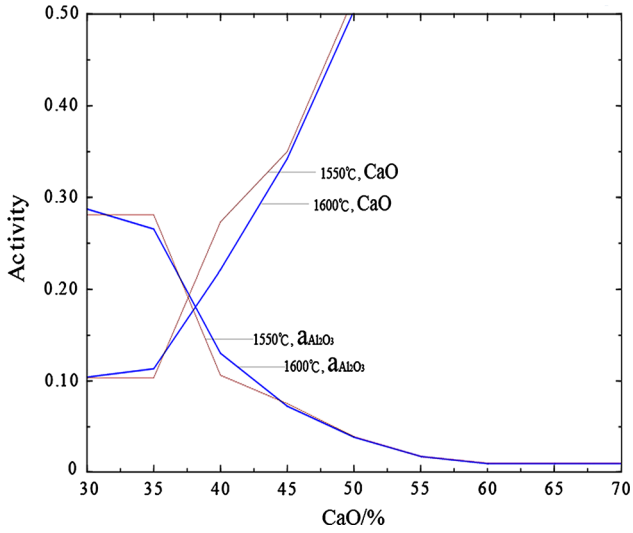

Fig. 3—CaO and Al_2O_3 activities in usual range of calcium aluminates at 1823 K and 1873 K (1550 °C and 1600 °C) calculated by FactSage.

Table IV. Activities of CaO and Al_2O_3 in Calcium Aluminates

	This work, [1823 K (1550 °C)] FactStage		This work, [1873 K (1600 °C)] FactStage		Korousic[14] Gemun model		Fujisawa[15] Experiment	
Mass Pct CaO	a_{CaO}	$a_{Al_2O_3}$	a_{CaO}	$a_{Al_2O_3}$	a_{CaO}	$a_{Al_2O_3}$	a_{CaO}	$a_{Al_2O_3}$
35	0.103	0.281	0.113	0.265	0.05	0.5	0.05	0.61
40	0.273	0.106	0.221	0.130	0.11	0.3	0.18	0.17
41	0.288	0.099	0.245	0.118				
42	0.304	0.093	0.269	0.107				
43	0.319	0.086	0.294	0.095				
44	0.335	0.079	0.318	0.084				
45	0.350	0.075	0.342	0.072	0.14	0.13	0.30	0.08
46	0.384	0.068	0.374	0.079				
47	0.418	0.062	0.407	0.072				
48	0.455	0.051	0.433	0.050				
49	0.489	0.044	0.472	0.043				
50	0.520	0.039	0.504	0.038	0.36	0.038	0.53	0.027
51	0.558	0.035	0.555	0.042				
52	0.596	0.030	0.606	0.038				
53	0.635	0.026	0.658	0.034				
54	0.711	0.021	0.709	0.030				
55	0.788	0.017	0.760	0.017				
56	0.829	0.015	0.806	0.013	0.6	0.012	0.72	0.02
57	0.870	0.012	0.853	0.012				
58	0.910	0.010	0.899	0.011				
59	0.926	0.010	0.825	0.011				
60	0.945	0.010	0.942	0.010				
61	0.974	0.010	0.973	0.010				
62	0.992	0.010	0.992	0.009	1	0.005	1	0.01

II. INDUSTRIAL TESTS

The industrial tests were carried out for steel plate cold common (SPCC), a kind of Ca-treated, Al-killed steel during the CSP process in a steel plant in China. Its melting process is BOF-LF-RH (Calcium treatment)-CC. Its refining temperature during RH is about 1873 K (1600 °C), and its tundish is about 1823 K (1550 °C). A total of 12 heats of industrial tests were carried out. Steel samples after calcium treatment for 8 minutes, at the beginning of tundish and in casting slab, were taken to analyze the chemical composition as shown in Tables I and II. The contents of C and S were analyzed by a C/S analyzer. Other elements were analyzed by the ICP-AES method. In addition, steel samples during RH, tundish refining, and in casting slab, rolled steel were taken, and inclusions on their cross sections were detected by EPMA-EDS and SEM-EDS to obtain their chemical composition, morphology, size, *etc*.

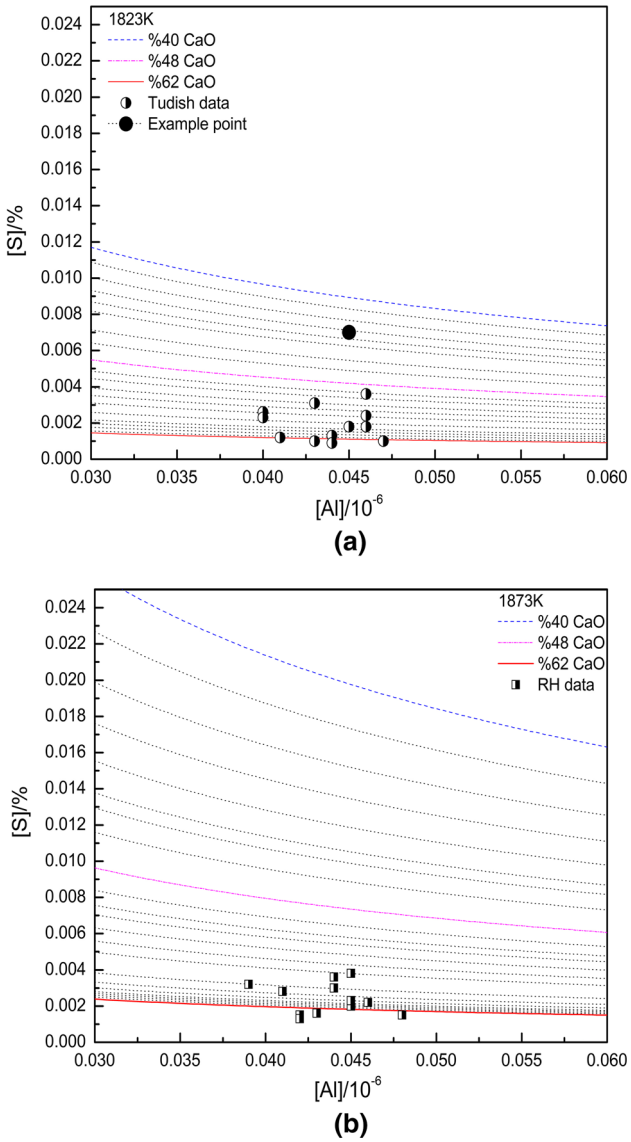

Fig. 4—Relationship of Al and S for precipitation of CaS in oxide-sulfide duplex inclusions at 1823 K and 1873 K (1550 °C and 1600 °C). (*a*) Relationship of Al and S for precipitation of CaS in oxide-sulfide duplex inclusions at 1823 K (1550 °C). (*b*) Relationship of Al and S for precipitation of CaS in oxide-sulfide duplex inclusions at 1873 K (1600 °C).

III. RESULTS AND DISCUSSION

A. *Thermodynamics for Precipitation of CaS-Bearing Inclusions*

The direct reaction between Ca and S can be represented as[6,7]:

$$\mathrm{Ca} + \mathrm{S} = \mathrm{CaS}$$

$$\Delta G_1^\circ = -542531 + 124.15T \qquad [1]$$

So the relationship between Ca and S for CaS precipitation can be expressed as:

$$[\text{Pct Ca}][\text{Pct S}] = \exp\left(-\frac{\Delta G_1^\circ}{\mathrm{RT}}\right)\frac{a_{\mathrm{CaS}}}{f_{\mathrm{S}} f_{\mathrm{Ca}}} \qquad [2]$$

where f_i is the activity coefficient of i (where i can be Ca, Al, and S) in liquid steel relative to the 1 wt pct standard state and a_i represents the activity of i (where i can be CaO, CaS, and Al_2O_3) relative to the pure solid standard state in this article. The activity coefficient is calculated by the first-order Wagner formalism expressed in Eq. [3] and e_i^j represents the first-order interaction coefficient of element j to i, whose values chosen in this work are shown in Table III.In particular, the values of some first-order interaction coefficients at 1823 K (1550 °C) that cannot be found now were replaced by the values at 1873 K (1600 °C). They were marked with *. The chemical composition of liquid steel in RH, tundish, and casting slab all were taken as follows: C 0.043; Si 0.19; Mn 1.82; Ni 0.2; P 0.01; S 0.001; Al_s 0.045; and O 0.0004. As the refining temperature may have a great effect on the

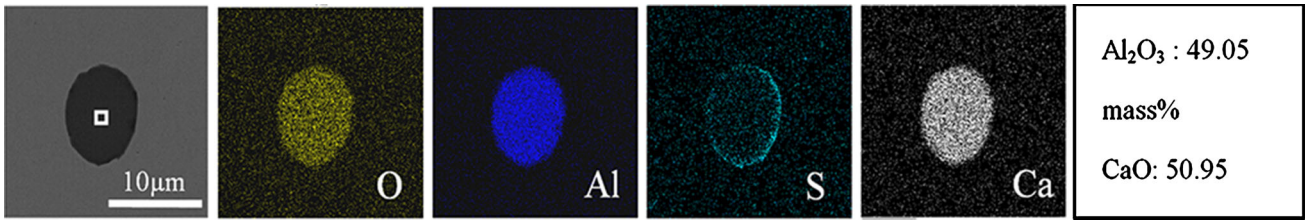

Fig. 5—SEM mapping of oxide-sulfur duplex inclusion in steel sample of tundish.

Table V. Standard Gibbs Free Energy of Reaction in Process of Calcium Treatment[4,16]

Reaction	ΔG°/J mol^{-1}
$3[Ca] + Al_2O_3 = 3CaO + 2[Al]$	$-664{,}577 + 40.45T$
$CaO + Al_2O_3 = CaO{\cdot}Al_2O_3$	$-18{,}000 - 18.83T$
$12CaO + 7Al_2O_3 = 12CaO{\cdot}7Al_2O_3$	$-73{,}053 - 207.53T$
$3CaO + Al_2O_3 = 3CaO{\cdot}Al_2O_3$	$-12{,}600 - 24.69T$

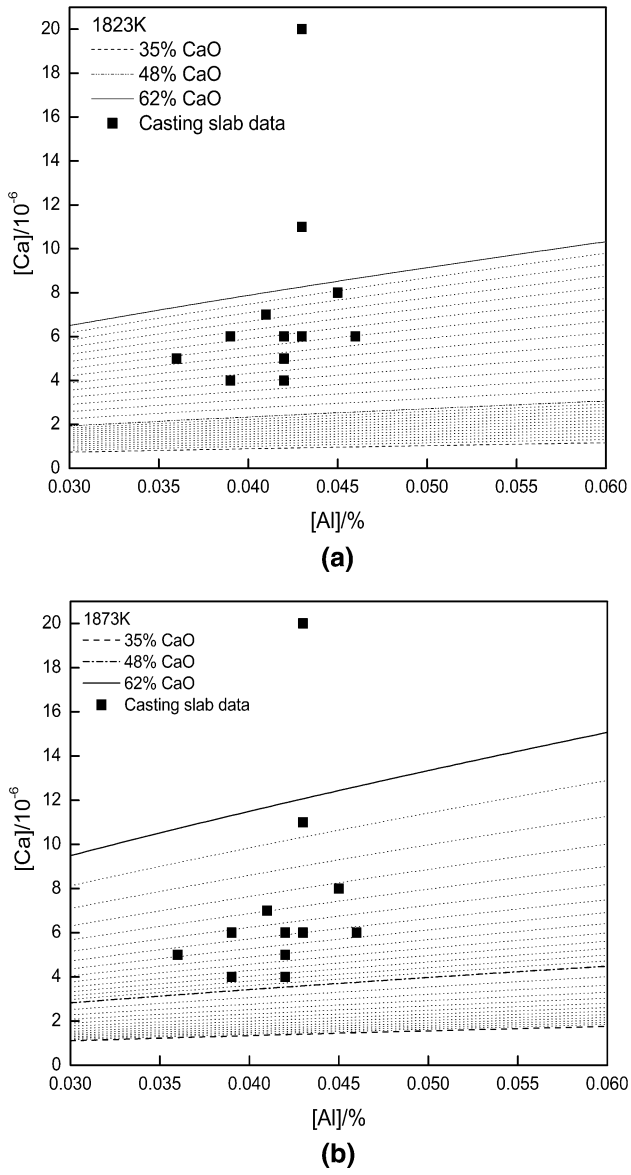

Fig. 6—Relationship between Ca and Al of different calcium aluminates at 1823 K and 1873 K (1550 °C and 1600 °C). (*a*) Relationship between Ca and Al of different calcium aluminates at 1823 K (1550 °C). (*b*) Relationship between Ca and Al of different calcium aluminates at 1873 K (1600 °C).

precipitation of CaS, thermodynamic analysis was performed at 1823 K and 1873 K (1550 °C and 1600 °C) for comparison:

$$\lg f_i = \sum e_i^j [\text{Pct } j] \qquad [3]$$

Table VI. Physical Properties of Inclusions[18]

Inclusion	Density (g cm^{-3})	Melting point [K (°C)]	Microhardness (kg mm^{-2})
Al_2O_3	3.96	2325 (2052)	3750
CA_6	3.28	2123 (1850)	2200
CA_2	2.91	2023 (1750)	1100
CA	2.98	1878 (1605)	930
$C_{12}A_7$	2.83	1728 (1455)	—
C_3A	3.04	1808 (1535)	—
CaO	3.34	2843 (2570)	400
CaS	2.50	2723 (2450)	—

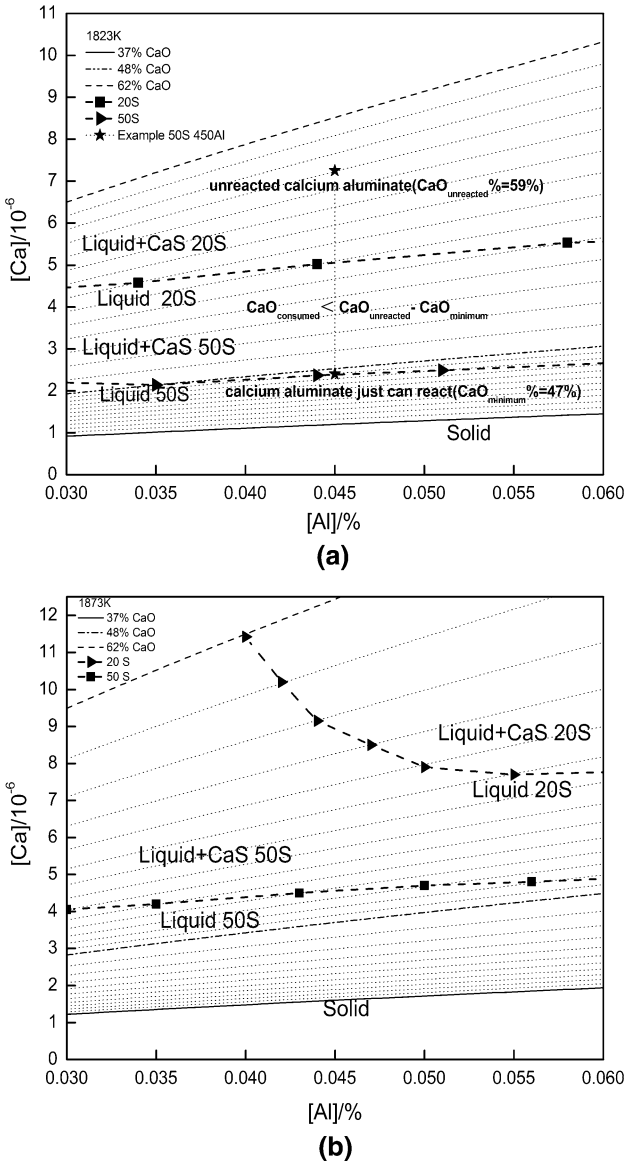

Fig. 7—Precipitated area of oxide-sulfide duplex inclusion when sulfur content is 20 and 50 ppm, respectively, at 1823 K and 1873 K (1550 °C and 1600 °C). (*a*) Precipitated area of oxide-sulfide duplex inclusion when sulfur content is 20 and 50 ppm at 1823 K (1550 °C). (*b*) Precipitated area of oxide-sulfide duplex inclusion when sulfur content is 20 and 50 ppm at 1873 K (1600 °C).

Figure 1 shows the relationship between Ca and S for the precipitation of CaS at 1823 K and 1873 K (1550 °C and 1600 °C). It was calculated by Eq. [2] and a_{CaS} was considered to be 1 relative to the pure solid standard. From Figure 1, it can be seen that the lower temperature, the easier it is to precipitate CaS. CaS cannot precipitate at 1873 K (1600 °C), and it more likely precipitates after the formation of calcium aluminates due to precipitation of CaS that needs a lower temperature.

Figure 2 shows SEM mapping of a special inclusion in which CaS was wrapped by calcium aluminates in steel samples after calcium treatment. Perhaps because of the high content of Ca and S in a small part of the molten steel after calcium treatment, Ca reacted directly with S precipitating CaS and then it was wrapped by calcium aluminates that formed later. It may prove that which forms first will be wrapped by the other between CaS and calcium aluminate. In the industrial tests, CaS were always found in the outer calcium aluminates and it may be because CaS precipitates after the formation of calcium aluminates due to its need for lower temperature. This matches with the thermodynamic calculation.

Due to the high activity of CaO in complete or overmodified calcium aluminates, CaO can react with dissolved Al, S in steel forming CaS and Al_2O_3. The chemical reaction is expressed as[2]:

$$3CaO + 2[Al] + 3[S] = 3CaS + Al_2O_3$$

$$\Delta G_2^\circ = -879760 + 298.73T \quad [4]$$

Thus, the mass fraction relationship between Al and S for the oxide–sulfide duplex inclusion is as follows:

$$[\text{mass pct Al}]^2[\text{mass pct S}]^3 = \exp\left(-\frac{\Delta G_2^\circ}{RT}\right)\frac{a_{CaS}^3 a_{Al_2O_3}}{a_{CaO}^3 f_S^3 f_{Al}^2} \quad [5]$$

Since there are not enough available experimental data, the thermodynamic software FactSage was used for estimating the activities of CaO and Al_2O_3 in calcium aluminates, and Figure 3 shows the results of calculation by FactSage. Table IV allows for the comparison from this work and previous researches.The calculated activities are in good agreement with the experimental value of Fujisawa.[15] The activities of CaO and Al_2O_3 of other calcium aluminates used in this thermodynamic analysis are also listed in Table IV. a_{CaS} was considered to be 1 relative to the pure solid standard.

Figure 4 shows the relationship between Al and S for the precipitation of CaS with various calcium aluminates at 1823 K and 1873 K (1550 °C and 1600 °C). The curves were calculated by Eq. [5]. In particular, more calcium aluminates were considered in Al-S equilibrium and the calculation became more accurate. For example, in Figure 4(a), other researchers[2,4,5] may consider that CaS will precipitate when Al is 0.045 pct and S reaches about 0.0045 pct for the example point. But in this article, with the same example point, when Al is 0.045 pct, CaS cannot precipitate until S reaches 0.0072 pct at least. It can be seen that the lower temperature, the easier it is to precipitate CaS-bearing inclusion from the comparison between (a) and (b) of Figure 4. In addition, Al has little effect on the precipitation of CaS-bearing inclusion, whereas S strongly influences the precipitation of CaS-bearing inclusion. The possibility of precipitating CaS increases with S content. Oxide-sulfur duplex inclusion is shown in Figure 5, and its characteristic is that CaO, Al_2O_3, and CaS mix in the outer layer of calcium aluminate inclusion.

For establishing the precipitation-area diagram of oxide-sulfide duplex inclusion, the process of calcium treatment was also researched. Because dissolved oxygen is very low in Al-killed steel when Ca is added to the liquid steel, the direct reaction between calcium and dissolved oxygen is deemed to be very few and it is ignored in this article. Thus, calcium treatment can be described by the following sets of chemical reactions:

$$x[Ca] + x/3Al_2O_3 = xCaO + 2/3x[Al] \quad \text{where } 0 < x \leq 1 \quad [6]$$

$$xCaO + (1-x)Al_2O_3 = (CaO)_x(Al_2O_3)_{1-x} \quad \text{where } 0 < x \leq 1 \quad [7]$$

Rearrangement of Eqs. [6] and [7] yields the following reaction:

$$x[Ca] + \left(1 - \frac{2}{3}x\right)Al_2O_3 = (CaO)_x(Al_2O_3)_{1-x} + \frac{2}{3}x[Al] \quad \text{where } 0 < x \leq 1 \quad [8]$$

The standard Gibbs free energy of Eq. [8] can be calculated by the data of Table V according to a specific response. $a_{(CaO)_x(Al_2O_3)_{1-x}}$ and $a_{Al_2O_3}$ were considered to be 1 using a pure substance as the standard state, so the mass fraction relationship between Ca and Al is as follows:

$$[\text{Al pct}]^{\frac{2}{3}x}/[\text{Ca pct}]^x = \exp(-\Delta G_3^\circ/RT)\frac{f_{Ca}^x}{f_{Al}^{\frac{2}{3}x}} \quad [9]$$

Figure 6 shows Ca-Al equilibrium with various calcium aluminates in which the mass fraction of CaO occupy 35 to 62 pct at 1823 K and 1873 K (1550 °C and 1600 °C). The curves of CA, $C_{12}A_7$, and C_3A were calculated by Eq. [9]. Other curves of calcium aluminates were calculated by adding the curves of CA, $C_{12}A_7$, and C_3A in proportion.

It needs about 40 minutes for the reaction of calcium treatment to reach equilibrium under the condition of having slag.[17] So the contents of Ca and Al at tundish station (as shown in Figure 6(b)) do not agree with the thermodynamic calculation at 1873 K (1600 °C) because the equilibrium time is not enough. In

consideration of dissolved Ca, the content is lower than that of total Ca, and the thermodynamic calculation of Ca-Al equilibrium at 1823 K (1550 °C) agrees well with the test data (as shown in Figure 6(a)) because the equilibrium time (10 minutes at RH and 30 minutes at tundish) for calcium treatment is enough.

Ca-Al equilibrium and Al-S equilibrium can be reached at the same time; therefore, Ca-Al equilibrium and Al-S equilibrium were combined in this article. In Figure 4, by fixing sulfur content at 20 and 50 ppm respectively, several intersections can be achieved on partial Al-S equilibrium curves. Then plugging these intersections into the corresponding Ca-Al equilibrium curves in Figure 6 and connecting the dots, the area above the line is the precipitated area of oxide-sulfide duplex inclusion and the area below the line is the area of liquid calcium aluminates. Figure 7 was obtained by this method.

Figure 7 shows the precipitation area of oxide-sulfide duplex inclusion at 1823 K and 1873 K (1550 °C and 1600 °C). It is observed that both S content and the temperature have significant impact on the precipitation of CaS. The lower the temperature and the higher the S content, the easier it is to precipitate oxide-sulfide duplex inclusion.

Figure 8 shows an unreacted core model of evolution of the $CaO\text{-}Al_2O_3$ system into the $CaO\text{-}Al_2O_3\text{-}CaS$ system. In Figure 8, the Reaction [4] in the reacting layer continues until CaO in the layer cannot react with [Al] and [S] from the liquid steel. The C-A-S layer is a stable layer, and it cannot react with [Al] and [S] again assuming S and Al contents in the liquid steel do not change in the process of Reaction [4]. In addition, it is deemed that CaO, Al_2O_3, and CaS cannot diffuse in the whole inclusion due to concentration difference, which means they are all still in the process of Reaction [4]. In the model, unreacted CaO and Al_2O_3 of calcium aluminates that involved Reaction [4] as well as CaS and Al_2O_3, which generated in Reaction [4] make up the stable C-A-S layer at last. So, the mass fraction of CaS in the stable C-A-S layer can be estimated and predicted by Eq. [10]:

$$\text{CaS pct} = \frac{\text{CaS}_{\text{generated}}\ \text{pct}}{(\text{CaO}_{\text{unreacted}}\ \text{pct} - \text{CaO}_{\text{consumed}}\ \text{pct}) + (\text{Al}_2\text{O}_{3_{\text{unreacted}}}\ \text{pct} + \text{Al}_2\text{O}_{3_{\text{generated}}}\ \text{pct}) + \text{CaS}_{\text{generated}}\ \text{pct}} \quad \text{where } \text{CaO}_{\text{initial}}\text{pct} + \text{Al}_2\text{O}_{3\text{initial}}\text{pct} = 1 \quad [10]$$

The example in Figure 7(a) shows the meanings of $CaO_{unreacted}$ pct, $CaO_{consumed}$ pct, and $CaO_{minimum}$ pct. Specifically, $CaO_{consumed}$ pct is mass fraction of CaO, which is consumed in Reaction [4] and $CaS_{generated}$ pct is the mass fraction of CaS, which is generated in Reaction [4]. $CaO_{unreacted}$ pct is the mass fraction of CaO in calcium aluminate, which is about to begin to react with [Al] and [S]. The meanings of the subscripts of Al_2O_3 in Eq. [10] are the same with corresponding subscripts of CaO and CaS. According to the mass balance relationship of Reaction [4], $CaS_{generated}$ pct equals $1.29CaO_{consumed}$ pct and $Al_2O_{3generated}$ pct equals $0.61CaO_{consumed}$ pct. Since the quantity of CaS that is generated in Reaction [4] is small, and for the ease of calculation, CaS is considered to be Al_2O_3 when calculating the mass fraction or activity of CaO in the $CaO\text{-}Al_2O_3\text{-}CaS$ system:

$$\text{CaO}_{\text{minimum}}\ \text{pct} = \frac{\text{CaO}_{\text{unreacted}}\ \text{pct - CaO}_{\text{consumed}}\ \text{pct}}{(\text{CaO}_{\text{unreacted}}\ \text{pct} - \text{CaO}_{\text{consumed}}\ \text{pct}) + (\text{Al}_2\text{O}_{3_{\text{unreacted}}}\ \text{pct} + \text{Al}_2\text{O}_{3_{\text{generated}}}\ \text{pct}) + \text{CaS}_{\text{generated}}\ \text{pct}} \quad \text{where } \text{CaO}_{\text{initial}}\ \text{pct} + \text{Al}_2\text{O}_{3\text{initial}}\ \text{pct} = 1 \quad [11]$$

$CaO_{minimum}$ pct can be known in Figure 7, and it is the minimum mass fraction of CaO in calcium aluminate that can react with [Al] and [S]. Rearrangement of Eqs. [10] and [11] yields Eq. [12]:

$$\text{CaS pct} = \frac{1.29(\text{CaO}_{\text{unreacted}}\ \text{pct} - \text{CaO}_{\text{minimum}}\ \text{pct})}{1 + 0.9\text{CaO}_{\text{initial}}\ \text{pct}} \quad [12]$$

Figure 9 shows the CaS capacity for certain calcium aluminates under the condition of fixing the content of Al and S. Figure 9 was calculated by Eq. [12]. The results of the calculation are coordinated with the test results of the inclusion (as shown in Figures 10 and 11). Although the quantity of generated CaS is not much, CaS has a significant effect on the physicochemical property of $CaO\text{-}Al_2O_3\text{-}CaS$ inclusion. This will be explained in the following section.

B. *Deformation During Rolling*

Figure 10 shows a series of calcium aluminates wrapped by pure CaS or oxide–sulfide duplex inclusion and their rolling directions toward right uniformly. Groups (a) to (d) in Figure 10 show deformation of A-CA_6-CA_2-CA wrapped by pure CaS. In group (a) of Figure 10, due to the high melting point and high microhardness of Al_2O_3 (as shown in Table VI), no deformation occurs during the rolling process.The CaS layer of it was torn but not separated from the Al_2O_3 core. In group (b) of Figure 10, which is similar to group (a), the CaS layer was torn. But there is a little difference, a small angle of the inclusion was stripped. It may because the microhardness of CA_6 (as shown in Table V) is lower than Al_2O_3 and the microhardness is not enough to make the whole inclusion keep from being not broken. If the microhardness of the inclusion core falls further and the plasticity of the inclusion core is not enough, the whole inclusion may be crushed down during the rolling process. As expected, the inclusion of CA_2 wrapped by CaS was crushed down (as shown in group (c1) of Figure 10) due to its lower microhardness and insufficient plasticity. But when the pure CaS layer becomes thicker, it can prevent CA_2 from being crushed (as shown in group (c2) of Figure 10). With the decreasing of the microhardness, the plasticity of the inclusion will increase, and when it increases to some extent, the inclusion will have a certain deformation ability to protect itself against the pressure and shear stress generated during the rolling process. In group (d) in Figure 10, the inclusion of CA wrapped by CaS deformed slightly and produced a pointed tail because of the deformation. This illustrates that the inclusion of CA wrapped by CaS has a certain plastic yielding ability. The CaS layer of the inclusion was not broken possibly because deformation of the CA core decreased the impact force. The melting point of CA is about 1873 K (1600 °C), and it can be a demarcation point of beginning to have a plastic yielding ability for calcium aluminates. In group (e) in Figure 10, the shell of the inclusion is oxide–sulfide duplex inclusion and the composition of the inclusion core is close to $C_{12}A_7$. It can be seen that both the shell and the core of the inclusion had a strong plastic yielding ability and almost deform uniformly. In general, the melting point has a corresponding relation to plastic yielding ability for the same kind of inclusion. The lower the melting point, the better deformation performance the inclusion has. The melting point of the calcium aluminates core is about 1500 K (1227 °C) lower than 1873 K (1600 °C) and that of the shell is about 1800 K (1527 °C). So the core should have plastic yielding ability and the shell did not prevent its plastic deformation. In oxide-sulfide duplex inclusion, the melting point of the shell is always higher than the core because of the joining of CaS. So if CaS in the oxide-sulfide duplex shell becomes more, the shell may prevent the plastic deformation of the whole inclusion. In group (f) in Figure 10, the shell of the inclusion is also oxide–sulfide duplex inclusion and composition of the inclusion core is close to C_2A. The inclusion is no plastic deformation. The melting point of the core is about 1673 K (1400 °C) lower than 1873 K (1600 °C) and that of the shell is about 1910 K (1637 °C). Because of the high melting point of the shell and plastic deformation ability of the core, it can be believed that the shell prevents the plastic yielding of the whole inclusion. Oxide–sulfide duplex shells like (e) and (f) type of shells were located in the CaO-Al_2O_3-CaS isothermal section calculated by Factsage (as shown in Figure 11). It can be found that there is a clear dividing line between the two kinds of shell. According to this line and the corresponding relation between melting point and plastic deformation, the plastic deformation region of oxide–sulfide duplex inclusion was roughly confirmed. Zone ① in Figure 11 can be the plastic deformation region. It can be seen that CaS has a

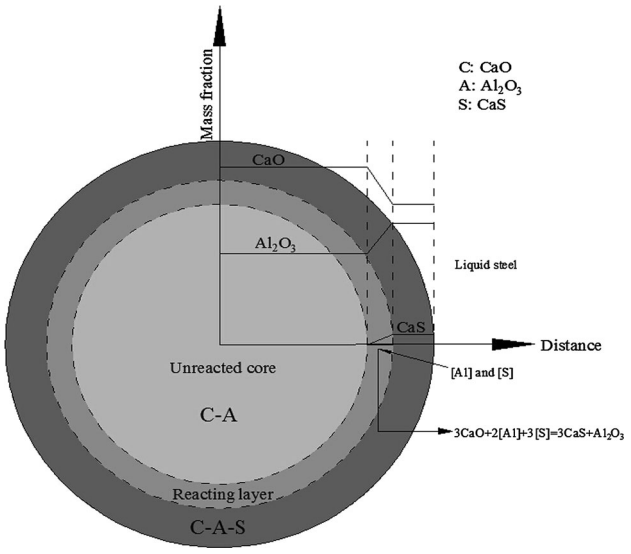

Fig. 8—Unreacted core model of evolution of CaO-Al_2O_3 system into CaO-Al_2O_3-CaS system.

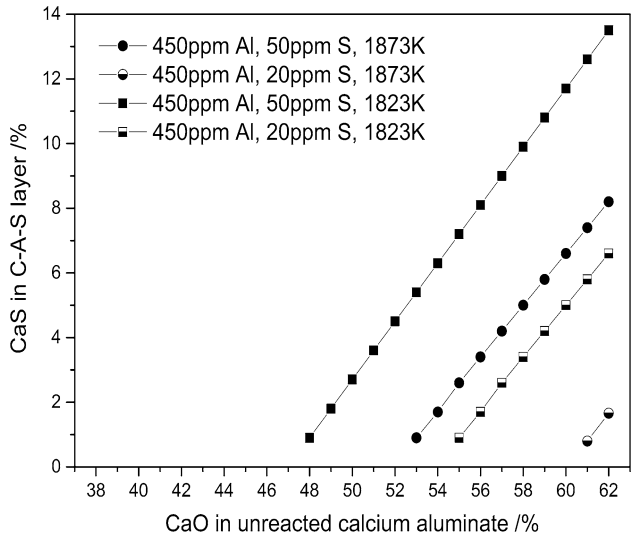

Fig. 9—Mass fraction of CaS in CaO-Al_2O_3-CaS inclusions when Reaction [4] reach equilibrium under different conditions.

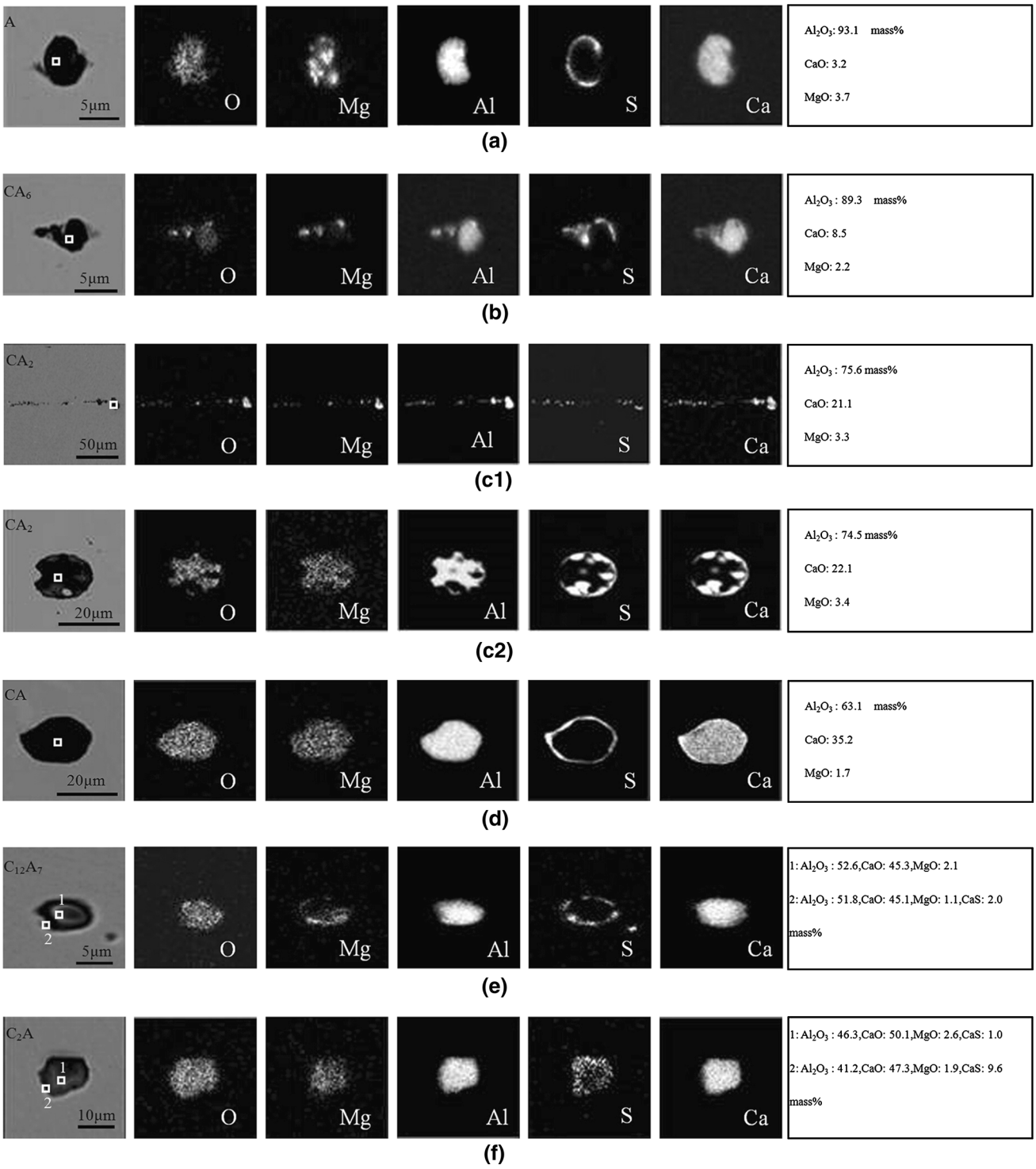

Fig. 10—EPMA mapping of CaS-bearing inclusions. (*a*) EPMA mapping of A wrapped by CaS. (*b*) EPMA mapping of CA_6 wrapped by CaS. (*c1*) EPMA mapping of CA_2 wrapped by CaS. (*c2*) EPMA mapping of CA_2 wrapped by CaS. (*d*) EPMA mapping of CA wrapped by CaS. (*e*) EPMA mapping of $C_{12}A_7$ wrapped by oxide-sulfide duplex inclusion. (*f*) EPMA-mapping of C_2A wrapped by oxide-sulfide duplex inclusion.

significant influence on the melting point and plastic deformation ability of the oxide-sulfide duplex inclusion. A small quantity of CaS may make the oxide–sulfide duplex shell lose plastic deformation ability due to the mushroom of the melting point.

By summarizing this inclusion observation, the process of calcium treatment is a softening process of modified inclusion. With the core of CaS-bearing inclusions changing in A-CA_6-CA_2-CA-$C_{12}A_7$ or C_2A, the deformation of the inclusions core varies with a route of no

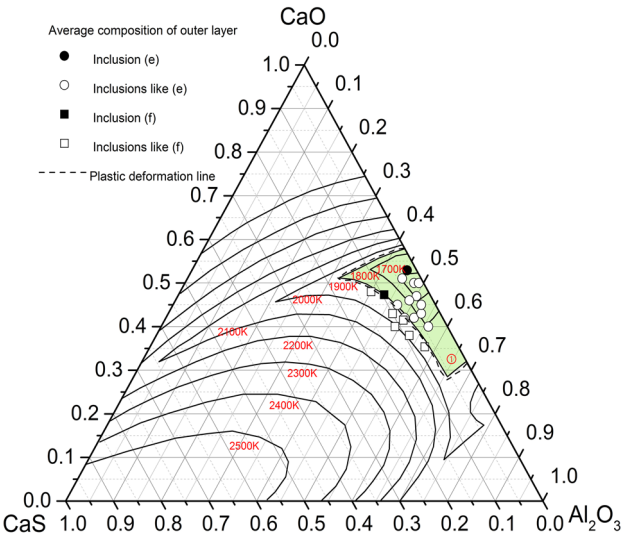

Fig. 11—CaO-Al_2O_3-CaS isothermal section diagram.

deformation-low brittleness-brittleness-little deformation-plastic deformation. But when these calcium aluminates are wrapped by pure CaS or oxide-sulfide duplex shell, their deformation ability may change. The deformations of low-modified calcium aluminates wrapped by pure CaS have different degrees of harm. A pure CaS layer, especially the thick one, has some protective and cushioning effect to calcium aluminates. An oxide-sulfide duplex shell contains less CaS and does not prevent plastic yielding of whole inclusion. When an oxide–sulfide duplex shell contains more CaS in the outer layer, it will lose the plastic yielding ability and even prevent the plastic deformation of whole oxide-sulfide duplex inclusion due to its high melting point. Therefore, it is important to modify Al_2O_3 inclusion in the proper range and to control the content of S in liquid steel to avoid or reduce the negative effects of CaS-bearing inclusions.

IV. CONCLUSIONS

Thermodynamics for the formation mechanism of CaS-bearing inclusions indicates that the refining temperature is very important to the precipitation of two types of CaS. The lower the temperature, the easier it is to precipitate CaS. One practical precipitation-area diagram of oxide-sulfide duplex inclusion was established under the condition of fixing S content. To explain the formation mechanism of oxide–sulfide duplex inclusion, an unreacted core model of evolution of the CaO-Al_2O_3 system into the CaO-Al_2O_3-CaS system was established. A mass fraction of CaS that was precipitated in Reaction [4] in a generated CaO-Al_2O_3-CaS inclusion can be calculated and predicted based on the precipitation-area diagram and the model.

The observation results for the deformation of six kinds of CaS-bearing inclusions during the rolling process indicate that oxide-sulfide duplex inclusion contains less CaS and does not prevent the plastic deformation of whole inclusion. But when CaS in the oxide-sulfide duplex inclusion layer accounts for more, it will make the melting point of the layer rise and prevent the plastic yielding of whole inclusion. The deformations of low-modified calcium aluminates wrapped by pure CaS have different degrees of harm. For some time, pure CaS has some protective and cushioning effect on calcium aluminates, keeping it intact and preventing it from stabbing the steel body. The plastic deformation region of oxide-sulfide duplex inclusion is preliminary confirmed. It is important to modify Al_2O_3 inclusion to the proper degree and to decrease the S content in liquid steel to avoid or reduce the negative effects of CaS-bearing inclusions.

ACKNOWLEDGMENT

The authors acknowledge National Natural Science Foundation of China (No. 51434004, U1435205) for the financial support.

OPEN ACCESS

REFERENCES

1. M.K. Sardar, S. Mukhopadhyay, U.K. Bandopadhyay, and S.K. Dhua: *Steel Res. Int*., 2007, vol. 78, pp. 136–40.
2. G. Ye, P. Jonsson, and T. Lund: *ISIJ Int*., 1996, vol. 36 (Supplement), pp. S105–08.
3. L. Holappa, M. Hämäläinen, M. Liukkonen, and M. Lind: *Ironmak. Steelmak*., 2003, vol. 30, pp. 111–15.
4. S.K. Choudhary and A. Ghosh: *ISIJ Int*., 2008, vol. 48, pp. 1552–59.
5. Jing. Guo, Shusen. Cheng, and Zijian. Cheng: *Steel Res. Int*., 2013, vol. 84, pp. 545–53.
6. G.K. Sigworth and J.F. Elliott: *Met. Sci*., 1974, vol. 8, pp. 298–310.
7. O. Kubaschewski, C.B. Alcock, and P.J. Spenscer: *Materials Chemistry*, 6th ed., Pergamon Press, Oxford, 1993, p. 169.
8. H. Suito and R. Inoue: *ISIJ Int*., 1996, vol. 36, pp. 528–36.
9. D.L. Sponseller and R.A. Flixm: *Trans. Metall. Soc. AIME*., 1964, vol. 230, pp. 876–80.
10. G.G. Mikhailov and A.G. Tyurin: *Izv. Akad. Nauk SSSR Met*., 1984, vol. 4, pp. 10–15.
11. R. Inoue and H. Suito: *Steel Res. Int*., 1994, vol. 65, pp. 403–09.
12. S.W. Cho and H. Suito: *Steel Res. Int*., 1994, vol. 34, pp. 265–69.
13. L.K. Liang, M.C. Che, and Y. Huai: *Metallurgical Thermodynamics and Kinetics*, Northeast Technology University Press, Shenyang, 1989.
14. B. Korousic: *Steel Res. Int*., 1991, vol. 62, pp. 285–89.
15. T. Fujisawa, C. Yamauchiand, and H. Sakao: *Iron and Steel Cong., 6th Int*. vol. 1, p. 201, ISIJ, Tokyo, 1990.
16. X.H. Huang: *Iron and Steel Metallurgy Principle*, 3rd ed., Metallurgical Industry Press, Beijing, 2012, p. 436.
17. T. Kimura and H. Suito: *Metall. Mater. Trans. B*, 1994, vol. 25B, pp. 33–42.
18. C.E. Cicutti, J. Madias, and J.C. Gonzalez: *Ironmak. Steelmak*., 1997, vol. 24, pp. 155–59.